Detection in Gamma-Distributed Nonhomogeneous Backgrounds

ÉRIC MAGRANER
NICOLAS BERTAUX
PHILIPPE RÉFRÉGIER
Fresnel Institute
France

We propose a new technique for target detection in RADAR range-Doppler maps in the presence of nonhomogeneous backgrounds with gamma-distributed fluctuations. This technique is based on a cell-averaging (CA) constant false alarm rate (CFAR) detection test for which the ratio threshold and the set of values involved in the detection test are adaptively optimized in order to improve the false alarm regulation and the detection probability in nonhomogeneous backgrounds. This technique is compared with standard detection techniques on a synthetic range-Doppler map which demonstrates the relevance of the proposed approach in nonhomogeneous gamma-distributed backgrounds.

Manuscript received December 13, 2007; revised October 20, 2008; released for publication March 3, 2009.

IEEE Log No. T-AES/46/3/937964.

Refereeing of this contribution was handled by C. Baker.

Authors' address: Institut Fresnel, Equipe Physique et Traitement d'Image, D. U. St. Jerôme, Marseille Cedex 20, 13397, France, E-mail: (nicolas.bertaux@fresnel.fr).

0018-9251/10/$26.00 © 2010 IEEE

I. INTRODUCTION AND BACKGROUND

A. Introduction

Target detection with large detection probability and constant false alarm rate in thermal noise and clutter[1] is of high practical interest in RADAR systems [1–5]. However, the control of the false alarm probability is difficult and subject to environmental conditions [6–9].

The cell-averaging (CA) constant false alarm rate (CFAR) processor, introduced by Finn and Johnson in 1968 [10] is the most popular CFAR processor adapted for gamma-distributed noise [11]. It uses a local noise power estimation from a reference region to compute an adaptive detection ratio threshold [10]. Gandhi and Kassam proved in [12] that the CA-CFAR processor is optimal in the sense that it maximizes the detection probability for a given false alarm probability for detecting Swerling I target [13–15] when the reference cells contain independent and identically distributed (IID) observations governed by an exponential distribution. Furthermore, in homogeneous gamma-distributed backgrounds, when the size of the reference region increases, the CA-CFAR processor performance tends towards the performance of the ideal detector [16], for which the mean value of the background and of the noise power is assumed to be a priori known. The ideal detector is based on the comparison with a ratio threshold of the pixel value under test divided by the statistical mean value of the background. Such a detector is not applicable in practice in general since the background statistical mean is rarely known a priori, but it can be considered as a reference to which other detectors can be compared. In the presence of nonhomogeneous backgrounds, the CA-CFAR performance is severely degraded, leading to excessive false alarms and/or target masking [16, 17]. Furthermore, it has been demonstrated that the choice of the reference region has a strong impact on the CA-CFAR performance [1, 18–20], and its optimization is difficult to realize in nonhomogeneous backgrounds. These difficulties, in general, result in nonhomogeneous backgrounds to non-CFAR of the CA-CFAR processor.

In this paper, we propose a new approach for target detection in range-Doppler maps acquired by airborne RADARs [2] which results in two-dimensional (2-D) maps that are analogous to images. More precisely, Swerling-I model target [13–15] is assumed embedded in 2-D nonhomogeneous gamma-distributed backgrounds of known order L. The proposed technique is based on a CA-CFAR detection test for which both the ratio threshold and the reference regions are adaptively optimized in order to improve the false

[1]The clutter refers to any undesired signal echo that is reflected back to the receiver.

alarm regulation rate and the detection probability. The ratio threshold value and the reference region shape are determined from an analysis of the CA-CFAR behavior in nonhomogeneous background. More precisely, it is shown that it is possible to determine the ratio threshold value that leads to an approximative CFAR and to select the reference region in order to optimize the detection probability when background values are known. We then demonstrate that a first rough estimation of the mean value of the background still allows one to improve the false alarm regulation and the detection probability in comparison with existing detection methods such as CA-CFAR [10], ordered statistics CFAR [21] and trimmed-mean (TM) CFAR [16] detection techniques.

After a brief introduction and description of the background and of the data model used in Section I, an original theoretical analysis of the standard CA-CFAR detector is performed in Section II. This analysis will allow one to understand the motivations of the new technique we propose and which is described in Section III. The results of this approach are presented in Section IV in comparison with other standard detection techniques, and the limits of the proposed approach is also investigated in this section. This analysis shows the key point for future improvements introduced in the perspectives that are discussed with the conclusion in Section V.

B. Background and Data Model

A range-Doppler map [2, 4] is obtained with a time-frequency analysis performed on the complex RADAR signals. This analysis results in a time-frequency map which is a 2-D image with one direction that corresponds to range and the other to Doppler. In general L time-frequency maps are acquired before processing and the squared modulus of these L maps are added providing a real valued intensity range-Doppler map. Each range-Doppler map is perturbed by fluctuations that are due to the thermal noise of the receiver and/or to clutter echoes. A usual approximation to describe these fluctuations is to consider that the complex RADAR signals are circular complex Gaussian random values with zero mean since time-frequency analysis is a linear operation. The acquisition of the L different time-frequency maps correspond to different times, and a fixed point in the scene is observed with small differences between the incident angles. A generally good approximation is thus to consider that the L different time-frequency maps correspond to independent realizations of circular complex Gaussian distributed fluctuations. Since the squared modulus of a circular complex Gaussian noise with zero mean is distributed with a gamma probability density function (pdf) of order 1, the addition of L maps leads to signal values that are distributed with a gamma pdf of order L.

In the following, the resulting intensity range-Doppler map is denoted $\mathbf{X}$ and, the order L of the gamma distribution is assumed known and equal to the number of time-frequency maps that are added. Furthermore, although the range-Doppler map $\mathbf{X}$ is a 2-D image with N cells, a 1-D lexicographical order of each cell's number is used in the following for simplicity reasons. More precisely, X_j is the value at cell j of the 2-D intensity range-Doppler map which is assumed to be distributed with a gamma pdf with mean m_j and order L (i.e., $X_j \sim \mathcal{G}(m_j, L)$) and which corresponds to independent random variables for different location j. The set $\{m_j\}_{j\in\{1\ldots N\}}$ defines the background mean value which is considered as a deterministic unknown variable. More precisely, different backgrounds that are described by different values $\{m_j\}_{j\in\{1\ldots N\}}$ can be observed in intensity range-Doppler maps. The goal of this paper is to develop an adaptive detection technique for each background. The values $\{m_j\}_{j\in\{1\ldots N\}}$ are thus nuisance parameters in the detection problem we consider.

The target echoes are modeled as Swerling-I targets [13–15] since their complex RADAR signals are assumed to be complex Gaussian distributed. In an intensity range-Doppler map, a target signal is assumed to result from independent successive time-frequency maps but fixed over a dwell used to form one time-frequency map. Furthermore, the target echo is assumed to be contained in a single cell. Then a target echo at the jth cell in the range-Doppler map is modeled by a random variable with a gamma pdf of order L and mean $m_j(1+S)$, where $S>0$ denotes the signal-to-noise ratio (SNR) of the target. In the following, this SNR is expressed in decibels ($S_{\text{dB}} = 10\log_{10}(S)$).

In conclusion, the values of the range-Doppler map X_j are written as the product of a deterministic background image with a random variable with a gamma pdf of unit mean and order L. The deterministic background image value is equal to m_j at cells where no target is present and to $m_j(1+S)$ at cells where a target is present. The pdf $f_X(x)$ of a cell value of mean m and order L can thus be written

$$f_X(x) \triangleq \frac{\mu^{-L}}{\Gamma(L)} x^{L-1} \exp\left(-\frac{x}{\mu}\right), \qquad x \geq 0$$

where $\mu = m/L$ and where the gamma function is $\Gamma(z) \triangleq \int_0^\infty t^{z-1}e^{-t}dt$.

II. ANALYSIS OF THE CA-CFAR PROCESSOR IN NONHOMOGENEOUS BACKGROUNDS

A. Introduction to the CA-CFAR Processor

A uniformly most powerful (UMP) detector can be obtained [12] when the mean background value m_j is

assumed known [16, 22]. Although this assumption is unrealistic, the analysis of this case is useful for the development of the proposed approach of this paper, and it is denominated the "ideal detector" in the following. In that case, the detection test at the cell i of value X_i consists in comparing the statistics X_i/m_i with a ratio threshold τ_i such that the following decisions are taken:

1) if $X_i/m_i > \tau_i$ a target is detected,
2) if $X_i/m_i < \tau_i$ no target is detected.

The false alarm probability P_{fa} is the probability to detect a target when no target is present while the detection probability P_d is the probability to detect a target when a target is indeed present. The detector based on the test X_i/m_i leads to the false alarm probability [11]

$$P_{fa}^{I}(\tau_i, m_i, L) = \Gamma(L\tau_i, L) \tag{1}$$

where $\Gamma(x,a)$ is the incomplete gamma function

$$\Gamma(x,a) = \int_x^{\infty} \frac{u^{a-1}}{\Gamma(a)} \exp(-u)du \tag{2}$$

and $\Gamma(a) = \Gamma(0,a)$ is the gamma function. The detection probability is

$$P_d^{I}(\tau_i, m_i, L, S) = \Gamma\left(\frac{L\tau_i}{1+S}, L\right). \tag{3}$$

To achieve a constant false alarm probability α fixed by the user, the ratio threshold τ_i is determined with (1) such that $P_{fa}^{I}(\tau_i, m_i, L) = \alpha$. In the following, the performance of this "ideal processor" is used as a benchmark and gives the best achievable detection probability for a given false alarm probability.

Since in real applications, the mean values m_i of the background are unknown, the ideal processor cannot be implemented in practice. The CA-CFAR processor [17, 10, 11] proposes an alternative by substituting m_i by the arithmetic mean $\bar{m}_{\omega_i}$ of reference cell values in a neighborhood ω_i of the cell i under test:

$$\bar{m}_{\omega_i} = \frac{1}{N_i} \sum_{j \in \omega_i} X_j \tag{4}$$

where N_i is the number of cells in ω_i. The reference region ω_i does not include the cell i under test in order not to bias the background value estimation when a target is present. The detection test thus consists of detecting a target if $X_i/\bar{m}_{\omega_i} > \tau_i$ and not detecting a target if $X_i/\bar{m}_{\omega_i} < \tau_i$.

In general the CA-CFAR detector is implemented with a sliding window divided in two or three mutually disjoint regions: 1) the target region χ_i, that contains the cell under test of value X_i, is limited to the cell under test; 2) the reference regions ω_is composed of the reference cells $\{j \in \omega_i,\ j \neq i\}$ and used to estimate the background value m_i (i.e., to determine $\bar{m}_{\omega_i}$); 3) additional guard cells can be added around the target region to prevent a biased noise power estimation if the target echo is not contained in a single cell. The size and shape of these regions are fixed a priori by the user.

In homogeneous backgrounds, the detection probability of the CA-CFAR processor is given by [11]

$$P_d^{\text{CA-CFAR}}(\tau_i, \omega_i, S) = 1 - \mathcal{I}\left(\frac{\frac{\tau_i}{N_i(1+S)}}{1+\frac{\tau_i}{N_i(1+S)}}, L, N_i L\right) \tag{5}$$

where $\mathcal{I}(x,a,b)$ is the regularized Beta function [23, 24] defined by $\mathcal{I}(x,a,b) = \mathcal{B}_{\mathcal{I}}(x,a,b)/\mathcal{B}(a,b)$, which is thus the ratio of the incomplete Beta function $\mathcal{B}_{\mathcal{I}}(x,a,b) = \int_0^x u^{a-1}(1-u)^{b-1}du$ with the Beta function which is defined by $\mathcal{B}(a,b) = \mathcal{B}_{\mathcal{I}}(1,a,b)$. The false alarm probability is obtained with fixing $S = 0$:

$$P_{fa}^{\text{CA-CFAR}}(\tau_i, \omega_i) = 1 - \mathcal{I}\left(\frac{\frac{\tau_i}{N_i}}{1+\frac{\tau_i}{N_i}}, L, N_i L\right). \tag{6}$$

To achieve a constant false alarm probability α which is fixed by the user, the ratio threshold τ_i is determined with (6) such that $P_{fa}^{\text{CA-CFAR}}(\tau_i, \omega_i) = \alpha$.

B. CA-CFAR Performance in Nonhomogeneous Backgrounds

In homogeneous backgrounds, the detection probability increases with the number of cells in the reference region and tends asymptotically towards the detection probability of the ideal processor described above. However, the CA-CFAR suffers an ineffective false alarm regulation on nonhomogeneous backgrounds [16]. We analyze in this subsection the behavior of the CA-CFAR processor in nonhomogeneous gamma-distributed backgrounds with Swerling-I target model. This analysis is useful to understand the motivations of the technique that is proposed in the next section. For that purpose, the expression of the detection and false alarm probabilities of the CA-CFAR processor have been determined (see Appendix):

$$P_d^{\text{CA}}(\tau_i, \omega_i, S) = C \sum_{k \geq 0} \delta_k \left[1 - \mathcal{I}\left(\frac{\frac{\tau_i}{N_i}\frac{\tilde{m}}{m_i(1+S)}}{1+\frac{\tau_i}{N_i}\frac{\tilde{m}}{m_i(1+S)}}, L, N_i L + k\right)\right] \tag{7}$$

where

$$\tilde{m} \triangleq \min_{j\in\omega_i}(m_j)$$

$$C = \prod_{j\in\omega_i}\left(\frac{\tilde{m}}{m_j}\right)^L \tag{8}$$

$$\delta_{k+1} = \frac{L}{k+1}\sum_{l=1}^{k+1}\left[\sum_{j\in\omega_i}\left(1-\frac{\tilde{m}}{m_j}\right)^l\right]\delta_{k+1-l}$$

$$\delta_0 = 1.$$

It appears that the detection probability $P_{\mathrm{d}}^{\mathrm{CA}}(\tau_i,\omega_i,S)$ is a function of the reference region through $m_i, \{m_j\}_{j\in\omega_i}$ and N_i. Thus, for the sake of clarity, it is also written $P_{\mathrm{d}}^{\mathrm{CA}}(\tau_i,\omega_i,S) = P_{\mathrm{d}}^{\mathrm{CA}}(\tau_i,m_i,\{m_j\}_{j\in\omega_i},N_i,S)$. The false alarm probability expression can be obtained taking $S = 0$:

$$P_{\mathrm{fa}}^{\mathrm{CA}}(\tau_i,\omega_i) = P_{\mathrm{fa}}^{\mathrm{CA}}(\tau_i,m_i,\{m_j\}_{j\in\omega_i},N_i) = P_{\mathrm{d}}^{\mathrm{CA}}(\tau_i,m_i,\{m_j\}_{j\in\omega_i},N_i,S=0). \tag{9}$$

Equations (7) and (9) determine the exact performance of the CA test in nonhomogeneous gamma-distributed backgrounds with order L. However, the physical situation is analogous to the one of the ideal processor since (9) needs that the mean background values m_i are known, which does not correspond to the realistic case we propose to analyze in this paper.

It is however interesting to analyze the obtained performance with the detection test $X_i/\bar{m}_{\omega_i}$ when the ratio threshold is determined with (9) with the background mean values m_i and $\{m_j\}_{j\in\omega_i}$ so that the false alarm probability is equal to α. In that case the false alarm probability is perfectly regulated, and one can analyze the influence of the shape and of the size of ω_i on the evolution of the probability of detection.

For that purpose, different numerical simulations have been performed on the background of mean value m_j shown in Fig. 1. Reference regions $\omega_i(j)$ with $j \leq 10$ are homogeneous while they become nonhomogeneous when $j > 10$. The target is located at cell $i = 0$ (represented with an arrow in Fig. 1) and has an SNR equal to 7 dB. For each reference region $\omega_i(j)$ the ratio threshold is fixed so that the false alarm probability α is equal to 10^{-4} and the probability of detection is shown in Fig. 1 as a function of the reference region size j.

It can be observed that when $j \leq 10$, the detection probability increases with j. This behavior is easily understandable since, in that case, the reference regions correspond to homogeneous backgrounds. On the contrary, when j becomes larger than 10, the detection probability still increases when $j \leq 12$, reaches a maximum value when $j = 12$, and finally it decreases for $j > 12$. The decrease of the detection probability clearly illustrates the influence

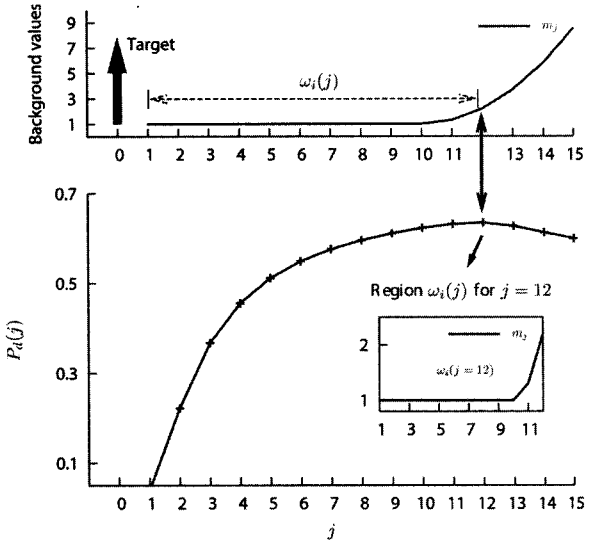

Fig. 1. Evolution as function of j of detection probability of detection test $X_i/\bar{m}_{\omega_i}$ for perfectly regulated false alarm probability ($\alpha = 10^{-4}$, $S_{\mathrm{dB}} = 7$ dB, $L = 4$).

of nonhomogeneous backgrounds on the detection performance. This simple simulation shows that for a false alarm probability equal to 10^{-4}, the detection probability reaches a maximum value when the reference region is nonhomogeneous.

In the next section, we propose to determine an optimal reference region and ratio threshold using (7) and (9) but with a rough estimation of the background mean value since it is not available in real situations.

III. DESCRIPTION OF THE PROPOSED DETECTION TECHNIQUE

A. General Structure of the Proposed Technique

The general structure of the proposed detection technique is based on a CA test and a reference region selection method, and it is denoted CARRS processors in the following. As for the CA-CFAR processor, the detection consists of comparing a statistical test with a ratio threshold. This statistical test is equal to the ratio of the value X_i of the cell under analysis to an estimation m_i^s of the background mean value m_i in a reference region ω_i^s determined in order to optimize the detection probability for a fixed false alarm rate. However, such an optimization is rigorously possible with (9) and (7) only if the mean value m_i and the target SNR S are known. This optimization can be nevertheless approximated if the mean values m_i, $\{m_j\}_{j\in\omega_i}$ in (9) and (7) are substituted by estimated mean value $\hat{m}_i$ and $\{\hat{m}_j\}_{j\in\omega_i}$. Iterative techniques could have been implemented so to simultaneously estimate m_i, $\{m_j\}_{j\in\omega_i}$, and S, but this approach would lead to large computational time, and also no proof of its optimality has been proved.

We thus propose to demonstrate that the selection of the ratio threshold value based on (9) with a first

rough estimation of the background mean value and using a simpler procedure than optimizing the detection probability provided by (7) allows one to get a selection of the reference region ω_i^s which improves the detection probability and the regulation of the false alarm probability in comparison to existing techniques. The different steps of the proposed technique are described in the following.

B. First Rough Estimation of the Background Mean Value

It is demonstrated in the following that a simple and fast estimation method based on a Gaussian filter is sufficient to improve the detection performance in nonhomogeneous backgrounds. The proposed technique is similar to the one developed in [25]. The considered Gaussian filter has a 2-D isotropic Gaussian impulse response excepted at the cell under test on which it is centered and where the impulse response is set equal to 0. This zero value is imposed in order to avoid biased background estimation that could result from the presence of a target. The amplitude of the filter is defined such that its integrated value is equal to one so that the estimation of the mean value is unbiased in homogeneous backgrounds. The width σ has been determined empirically in order to improve the regulation of the false alarm probability on the considered range-Doppler map (i.e., with numerical simulations) which has lead to $\sigma = 1.6$ cells. Since filtering is well adapted to additive noise, the filtering operation is applied on the logarithm of the cell values.

However, although considering the logarithm of the cell values transforms the gamma multiplicative noise into an additive noise, this additive noise does not have a symmetrical pdf. Consequently, the weighted mean estimation obtained with the Gaussian filter does not lead to an unbiased estimation of the background mean. Indeed, since X_i is assumed distributed with the gamma pdf $\mathcal{G}(m_i, L)$, the statistical mean value of $\ln(X_i)$ is equal to [26] $\ln(m_i) + \psi(L) - \ln(L)$ where $\psi(x) = (d/dx)\ln\Gamma(x)$ is the Digamma function. Thus, if $\hat{\eta}_i$ denotes the result of the filtering of the logarithm of the cell values, the following estimation of the background mean

$$\hat{m}_i = L\exp[\hat{\eta}_i - \psi(L)] \tag{10}$$

is used.

C. Threshold Determination

For any a priori reference region ω_i the ratio threshold value $\tilde{\tau}_i(\omega_i)$ that leads to an approximative value of the false alarm probability can be obtained with (9). Indeed, using the first rough estimation $\hat{m}_i$ provided by (10), it is possible to solve the following equation:

$$P_{\text{fa}}^{\text{CA}}(\tilde{\tau}_i(\omega_i), \hat{m}_i, \{\hat{m}_j\}_{j\in\omega_i}, N_i) = \alpha. \tag{11}$$

Numerically, the ratio threshold $\tilde{\tau}_i(\omega_i)$ is computed using a bi-section method [27] until $(P_{\text{fa}}^{\text{CA}}(\tilde{\tau}_i(\omega_i), \hat{m}_i, \{\hat{m}_j\}_{j\in\omega_i}, N_i) - \alpha)/\alpha$ is lower or equal to one percent. Of course this equation does not guarantee that the obtained false alarm probability will be equal to α since the mean values $\hat{m}_j$ considered in this equation are only rough estimations. It is nevertheless shown in the following that this approach improves the performance in comparison with the other tested technique in the false alarm probability regulation.

D. Reference Region Selection Technique

Formally, the detection probability can be optimized in nonhomogeneous backgrounds for a fixed false alarm probability. Indeed, the quantity provided by (7) can be maximized as a function of ω_i when the ratio threshold $\tilde{\tau}_i(\omega_i)$ obtained with (11) has been injected. This optimization allows us to determine the reference region ω_i^0 that maximizes

$$P_{\text{d}}^{\text{CA}}(\tilde{\tau}_i(\omega_i), \hat{m}_i, \{\hat{m}_j\}_{j\in\omega_i}, N_i, S) \tag{12}$$

which is obtained with (7) in which the mean values m_j have been replaced by their estimates $\hat{m}_j$. However, the result of such an optimization will be a function of the target SNR S which is a priori unknown. Furthermore, a search of the optimal reference region ω_i^0 over all the cells of the image would be very time consuming and probably of little interest if the obtained cells were not located around the cell under test. We thus propose to implement an optimization in two steps in order to introduce spatial constraints, to not have to assume any value for the SNR S, and to reduce the computational time.

1) *First Step of the Reference Region Selection*: The first step consists of determining a set of reference regions of cells that are in an a priori determined window around the cell i under test and finding values that are near the value of this cell.

Let $\Omega_i \subset \{1, \ldots, N_{\Omega_i}\}$ be a set of cells in a window (typically a set of $N_{\Omega_i} = 15 \times 15$ cells) centered on the cell i whose mean value $\hat{m}_i$ has been estimated with (10). The set of reference regions $\omega_i(R)$ is then determined as the 8-connected set of cells that are in Ω_i and that have estimated values $\hat{m}_j$ between $\hat{m}_i(1-R)$ and $\hat{m}_i(1+R)$ (see Fig. 2), i.e., such that

$$\forall \quad j \in \omega_i(R), \qquad \hat{m}_i(1-R) < \hat{m}_j < \hat{m}_i(1+R). \tag{13}$$

The connectivity of the reference region is ensured by a region-growing algorithm whose seed is the pixel under test and that aggregates the cells in Ω_i which verifies (13) (see Fig. 3). This approach is analogous

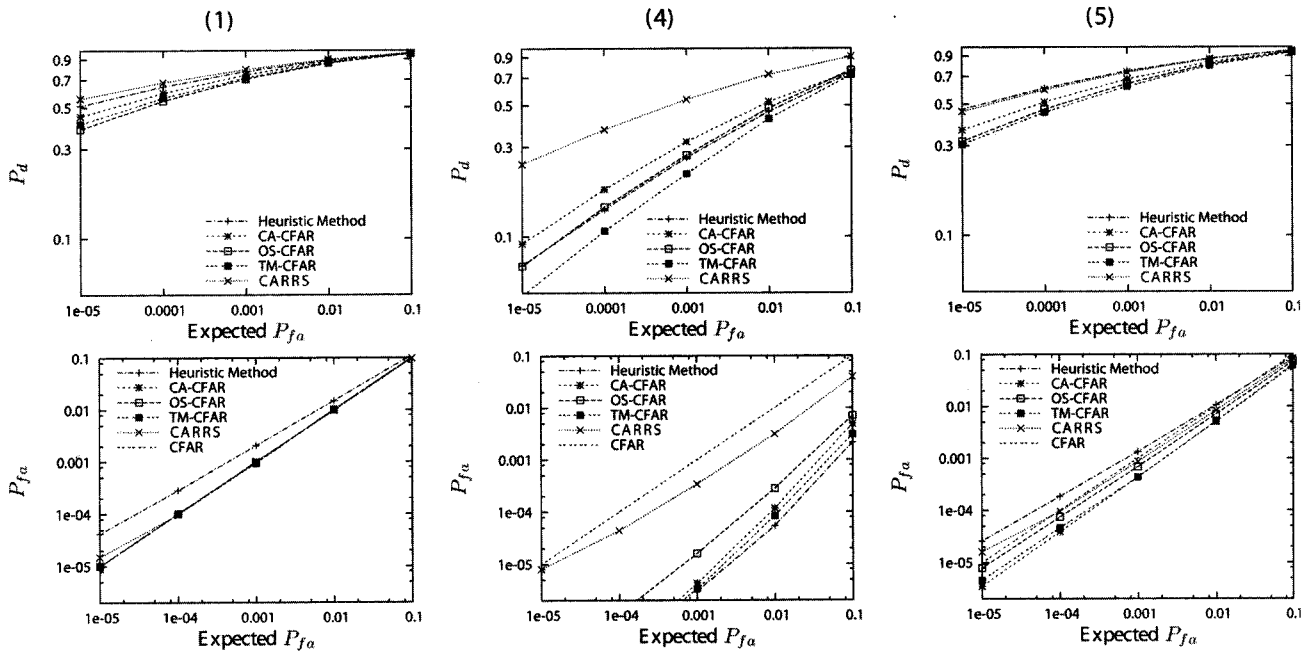

Fig. 5. Comparison of detection performance of CARRS processor with other well-known detection techniques for target numbers 1 (1), 4 (4), and 5 (5). For each column, at top, detection probability versus expected false alarm probability α and below, false alarm probability versus expected false alarm probability α.

probability in nonhomogeneous background with fluctuations distributed with a gamma pdf.

The computational time of the proposed method increases with the inhomogeneity of the region around the tested cell since it is mainly due to the time needed to select the reference region. Indeed, this selection requires a truncation of the infinite sums of (7) and (9). However, for a fixed accuracy on the performance, the truncation order has to be increased with the inhomogeneity of the region ω_i. For example, this time is smaller than 1 ms at location of target 1, approximatively equal to 1 ms at location of target 2, 6 ms at location of target 3, 18 ms at location of target 4, and 5 ms at location of target 5 with a standard computer (3.2 Ghz, linux 2.6.18, GCC 4.1.2).

C. Analysis of the CARRS Performance

The improvement of the performance of the CARRS processor in comparison with other well-known detection techniques has been demonstrated in the previous section. We propose in this subsection to analyze this approach more precisely.

We first report in Fig. 6 the performance of the CARRS processor when the limitations on the R values and on the pixel numbers of the reference regions discussed in the previous section are not implemented. It clearly appears that for target 4, which is embedded in a strongly nonhomogeneous background, the control of the false alarm rate is severely degraded without these constraints.

Furthermore, two main approximations have been considered in the development of the CARRS processor. The first one is the use of the first rough estimation $\hat{m}_i$ provided by (10) of the background value m_i in (7) and (9). The second one is the consequence of the minimization of (19) instead of the optimization of the detection probability which is used to automatically determine the reference region $\omega_i(R^s)$.

In the simulations the exact background mean value can be used in (7) and (9) to determine the ratio threshold $\tau_i(R)$ and for the reference region selection. The obtained modified version of the CARRS processor for which the reference region is determined with the exact background mean value, is denominated CARRS-KNHB processor in the following presented simulations. Since this processor uses the exact background mean value, only the limitation $R_{\max} = 0.6$ is applied. The performance of the ideal processor based on the comparison of the statistics X_i/m_i with a ratio threshold τ_i determined with (1) is also reported. Both the results of the CARRS-KNHB and of the ideal processors are presented in order to investigate the performance of the CARRS processor but cannot be implemented in real situations since they need the knowledge of the background values m_j.

The results obtained for targets 1 (homogeneous background), 4 and 5 are presented in the Fig. 6. It can be observed, as expected, that the CARRS-KNHB processor offers a perfect control of the false alarm rate. Moreover, the performance of the CARRS-KNHB processor are approximatively

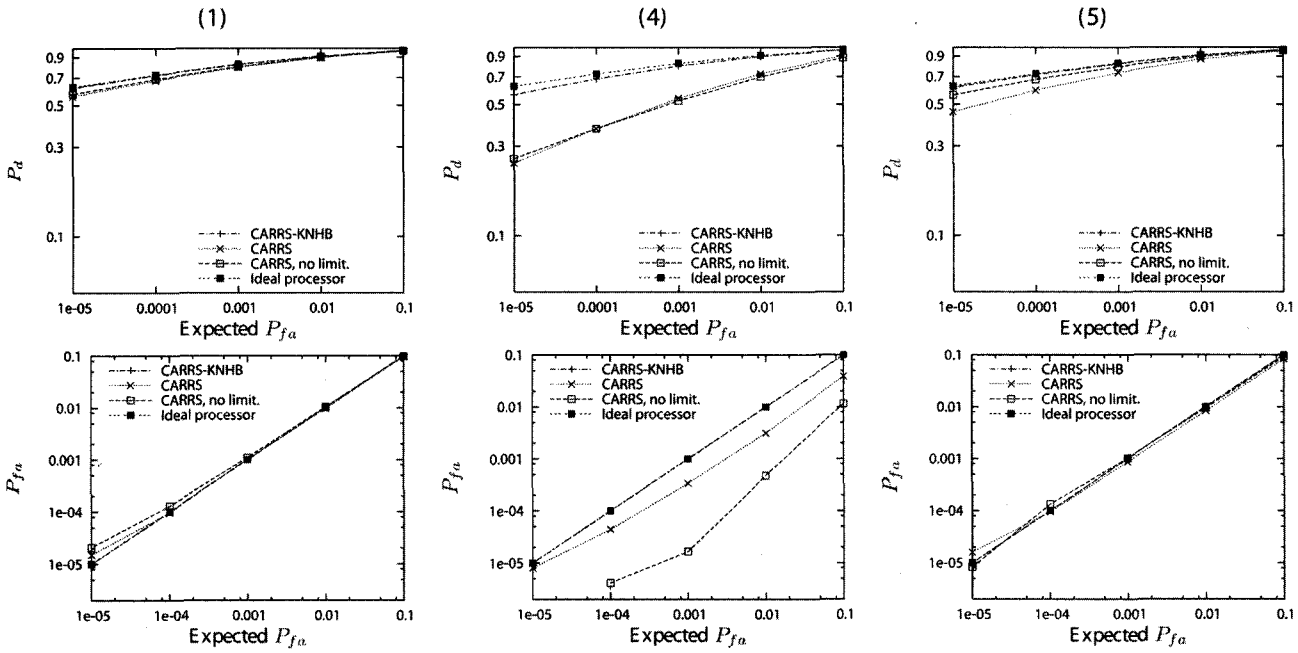

Fig. 6. Analysis of CARRS performance for target numbers 1 (1), 4 (4), and 5 (5). Modified version of CARRS processor for which reference region is determined with exact background mean value is denominated CARRS-KNHB processor. For comparison, performance of CARRS processor and performance of CARRS, no limit. are reported. The CARRS, no limit. stands for the CARRS processor when no constraint other than $R_{\max} = 0.35$ and reference region size smaller than 30 pixels are implemented. For each column, at top, detection probability versus expected false alarm probability α and below, false alarm probability versus expected false alarm probability α.

equal to the one of the ideal processor. This result demonstrates that the region selection technique is efficient, and most of the loss in performance of the CARRS processor is due to the first rough background estimation $\hat{m}_j$. This observation opens interesting perspectives.

V. CONCLUSIONS

The expressions of the CA test performance in nonhomogeneous backgrounds with fluctuations distributed with gamma pdfs have been presented for Swerling I target model. Using these expressions, we have proposed the CARRS detector in order to improve the regulation of the false alarm rate in unknown nonhomogeneous gamma-distributed backgrounds. A comparison of the performance of the proposed method with other detection processors (CA-CFAR, OS-CFAR, TM-CFAR) has been presented. This comparison has demonstrated that the CARRS detector offers a better control of the false alarm rate in nonhomogeneous background with good detection probability but at the expense of an increase in the computational cost. The results were obtained using a very simple background estimation method, and it has been shown that it is probably the main source of the present limitations of the CARRS approach. This result opens interesting perspectives. Indeed, since the CARRS detector improves the performance in comparison with standard technique in nonhomogeneous background, its improvement with a more precise background estimation is a challenging problem. Another motivating perspective is to reduce the computational cost of the proposed method for real-time applications.

Finally, the CARRS approach could also be generalized to nonhomogeneous backgrounds for which the orders of the gamma pdf is different for different cells or to other speckle model with non-gamma pdfs. It will be also interesting to access the effects of different types of nonhomogeneity and any limitations to the performance that can be achieved.

APPENDIX. CA TEST PERFORMANCE

This Appendix is organized as follows. First, the pdf of the random variable $\bar{m}_{\omega_i}$ is expressed as a single gamma-series (result obtained by Moschopoulos [35]). Secondly, the pdf of the random variable $X_i/\bar{m}_{\omega_i}$ is derived. Thirdly, the expression of the detection probability of the CA-CFAR processor in nonhomogeneous backgrounds is established.

Let us introduce Z_i the sum of the reference cell values X_j, $j \in \omega_i$:

$$Z_i \triangleq \sum_{j \in \omega_i} X_j = N_i \cdot \bar{m}_{\omega_i} \tag{22}$$

where $X_j \sim \mathcal{G}(m_j, L)$ and $\forall j \in \omega_i$, $m_j \in \mathbb{R}^+ \backslash \{0\}$, $L \in \mathbb{R}^+ \backslash \{0\}$, $N_i = \text{card}(\omega_i)$. Instead of $\bar{m}_{\omega_i}$, we use the

random variable Z_i, that is more convenient to use for the calculus.

A. The Density of Z_i

First we consider the pdf of Z_i. In 1985, Moschopoulos [35] derived an expression for the pdf of the sum of gamma variables:

$$f_{Z_i}(z_i) = C\sum_{k\geq 0}\frac{\delta_k z_i^{N_iL+k-1}e^{-z_i/\tilde{\mu}}}{\tilde{\mu}^{N_iL+k}\Gamma(N_iL+k)}, \qquad z_i \geq 0 \quad (23)$$

where $\tilde{\mu} = \tilde{m}/L$ and $\tilde{m}$, C, δ_k are defined in (8). We define the random variable W_i as

$$W_i \triangleq \frac{X_i}{Z_i} = \frac{X_i}{N_i \cdot \bar{m}_{\omega_i}}.$$

B. Probability Density Function of W_i

The pdf of W_i can be expressed as (see [31])

$$f_{W_i}(w_i) = \int_{-\infty}^{\infty}|z_i| f_{X_i}(w_i \cdot z_i) f_{Z_i}(z_i)dz_i.$$

Let X_i be a gamma random variable of mean m_i and order L; then

$$f_{W_i}(w_i) = \int_0^{\infty}\sum_{k\geq 0} g_k(z_i, w_i)dz_i$$

where

$$g_k(z_i, w_i) = z_i\frac{\mu_i^{-L}}{\Gamma(L)}(w_i z_i)^{L-1}\exp\left(-\frac{w_i z_i}{\mu_i}\right) \times C\frac{\delta_k z_i^{N_iL+k-1}e^{-z_i/\tilde{\mu}}}{\tilde{\mu}^{N_iL+k}\Gamma(N_iL+k)}$$

and $\mu_i = m_i/L$.

PROPOSITION 1 *The integration and the summation in the expression of f_{W_i} can be interchanged.*

PROOF In [35], it is proved that

$$f_{Z_i}(z_i) \leq C\frac{\tilde{\mu}^{-N_iL}}{\Gamma(N_iL)}z_i^{N_iL-1}\exp\left[-z_i\frac{1-b}{\tilde{\mu}}\right]$$

where

$$b \triangleq \max\left(\left\{1-\frac{\tilde{m}}{m_j}, j\in\omega_i\right\}\right).$$

Using this result, we obtain

$$\sum_{k\geq 0} g_k(z_i, w_i) \leq C\frac{\mu_i^{-L}\tilde{\mu}^{-N_iL}}{\Gamma(L)\Gamma(N_iL)}w_i^{L-1}z_i^{L+N_iL-1} \times \exp\left[-z_i\left(\frac{w_i}{\mu_i}+\frac{1-b}{\tilde{\mu}}\right)\right]. \quad (24)$$

Thanks to the dominated convergence theorem (see [32]), we establish the dominated convergence of $\sum_{k\geq 0} g_k(z_i, w_i)$. Then we can interchange the integration and the summation in the expression of f_{W_i}.

Introducing the Beta function (defined in Section IIA), we group together the terms depending on z_i and we get the following form for f_{W_i}:

$$f_{W_i}(w_i) = C\sum_{k\geq 0}\frac{\delta_k w_i^{L-1}}{\mu_i{}^L\mathcal{B}(L, N_iL+k)} \times \frac{1}{\left(\frac{w_i}{\mu_i}+\frac{1}{\tilde{\mu}}\right)^{L+N_iL+k}\tilde{\mu}^{N_iL+k}} \times \int_0^{\infty} h_{k,L,N_i,\mu_i,\tilde{\mu}}(z_i)dz_i$$

where $h_{k,L,N_i,\mu_i,\tilde{\mu}}(z_i)$ are the pdfs of gamma random variables of shape parameter $L+N_iL+k$ and of scale parameter $(w_i/\mu_i + 1/\tilde{\mu})^{-1}$. Then, the pdf of W_i is given by

$$f_{W_i}(w_i) = C\sum_{k\geq 0}\frac{\delta_k w_i^{L-1}}{\mu_i^L\mathcal{B}(L, N_iL+k)} \times \frac{1}{\left(\frac{w_i}{\mu_i}+\frac{1}{\tilde{\mu}}\right)^{L+N_iL+k}\tilde{\mu}^{N_iL+k}}, \qquad w_i \geq 0.$$

C. CA Test Performance

Using the expression of the pdf of W_i, we derive the expression of the CA test performance. For a ratio threshold τ_i, the probability of detection is defined as

$$P_{\mathrm{d}}^{\mathrm{CA}}(\tau_i, m_i, \{m_j\}_{j\in\omega_i}, N_i, S) = \int_{\tau_i/N_i}^{\infty} f_{W_i}(w_i)dw_i.$$

Let us note $\tau_{W_i} = \tau_i/N_i$ and $m_{i,S} = m_i(1+S)$ where S is the SNR. Substituting w_i by

$$x_i = \frac{w_i\frac{\tilde{m}}{m_{i,S}}}{1+w_i\frac{\tilde{m}}{m_{i,S}}}$$

the detection probability expression can be rearranged as:

$$P(W_i > \tau_{W_i} \mid H_1, m_i, \{m_j\}_{j\in\omega_i}, N_i, S) = \int_{\frac{\tau_{W_i}\tilde{m}/m_{i,S}}{1+\tau_{W_i}\tilde{m}/m_{i,S}}}^{1}\sum_{k\geq 0} e_k(x_i)dx_i$$

where the functions $e_k(x_i)$ are such that

$$e_k(x_i) = C\frac{\delta_k}{\mathcal{B}(L, N_iL+k)}x_i^{L-1}(1-x_i)^{N_iL+k-1}.$$

PROPOSITION 2 *The integration and the summation in the detection probability expression can be interchanged.*

PROOF Using the upper bound of δ_k defined in [35],

$$|\delta_k| \leq \frac{(N_i L)_k}{k!} b^k$$

and the following property holds:

$$\mathcal{B}(L, N_i L + k) = \frac{(N_i L)_k}{(L + N_i L)_k} \mathcal{B}(L, N_i L)$$

where $(a)_k$ is the Pochhammer symbol defined by $(a)_k \triangleq \prod_{i=0}^{k-1}(a+i)$ and $b \triangleq \max(\{1 - \tilde{m}/m_j,\ j \in \omega_i\}) \leq 1$. Then $B_k(x_i)$ exists such that

$$|e_k(x_i)| \leq B_k(x_i)$$

and

$$B_k(x_i) \triangleq C \frac{x_i^{L-1}}{\mathcal{B}(L, N_i L)} (1 - x_i)^{N_i L - 1} \frac{(L + N_i L)_k}{k!} [b(1 - x_i)]^k.$$

Moreover it can be proved that

$$B_k(x_i) \leq B_k^0 = B_k(x_0), \qquad x_0 = \frac{L-1}{L + N_i L + k - 2}.$$

Hence

$$\frac{B_{k+1}^0}{B_k^0} = \frac{(L + N_i L + k)}{(L + N_i L - 1)} \frac{b(1 - x_0)}{(k+1)}.$$

The d'Alembert theorem allows one to prove the convergence of the series B_k^0. It implies that $e_k(x_i)$ converges uniformly (Weierstrass' criterion [24]). Then the integration and summation can be interchanged in the detection probability expression (uniform convergence theorem, see [26]).

Dividing the integral in two parts and using the definition of the regularized Beta function (see Section IIA), we get

$$P_{\mathrm{d}}^{\mathrm{CA}}(\tau_i, m_i, \{m_j\}_{j \in \omega_i}, N_i, S) = C \sum_{k \geq 0} \delta_k \left[1 - \mathcal{I} \left(\frac{\frac{\tau_i}{N_i} \frac{\tilde{m}}{m_i(1+S)}}{1 + \frac{\tau_i}{N_i} \frac{\tilde{m}}{m_i(1+S)}}, L, N_i L + k \right) \right].$$

The numerical computation of the CA test performance expressions must be carefully studied. Particularly the truncation of the summation must be correctly realized to ensure accurate results.

For practical purposes, a bound for the truncation error $\varepsilon_K(\tau_i)$ can be obtained:

$$\begin{aligned} \varepsilon_K(\tau_i) &= P_{\mathrm{fa}}^{\mathrm{CA}}(\tau_i, m_i, \{m_j\}_{j \in \omega_i}, N_i) - P_{\mathrm{fa}}^{\mathrm{CA}^K}(\tau_i, m_i, \{m_j\}_{j \in \omega_i}, N_i) \\ &= C \sum_{k \geq K+1} \delta_k \left[1 - \mathcal{I} \left(\frac{\frac{\tau_i}{N_i} \frac{\tilde{m}}{m_i}}{1 + \frac{\tau_i}{N_i} \frac{\tilde{m}}{m_i}}, L, N_i L + k \right) \right] \\ &\leq C \sum_{k \geq K+1} \delta_k = 1 - C \sum_{k=0}^{K} \delta_k = \varepsilon_K(0) \end{aligned}$$

where $P_{\mathrm{fa}}^{\mathrm{CA}^K}(\tau_i, m_i, \{m_j\}_{j \in \omega_i}, N_i)$ is the sum of the first K terms of $P_{\mathrm{fa}}^{\mathrm{CA}}(\tau_i, m_i, \{m_j\}_{j \in \omega_i}, N_i) \triangleq P_{\mathrm{d}}^{\mathrm{CA}}(\tau_i, m_i, \{m_j\}_{j \in \omega_i}, N_i, S = 0)$.

ACKNOWLEDGMENT

The authors thank the Délégation Général de l'Armement (DGA) and the Centre National pour la Recherche Scientifique (CNRS) for supporting the Ph.D. thesis of Éric Magraner and Thales Airborne Systems for providing data. The authors would like to thank more particularly Alain Becker of Thalès Airborne Systems, Sébastien Paillardon and Jacques Blanc-Talon of the DGA.

REFERENCES

[1] Campbell, L. L.
Air-to-air RADAR modes for the CP-140 maritime patrol aircraft.
Ph.D. dissertation, Dept. of Systems and Computer Engineering, Ottawa-Carleton Institute for Electrical Engineering, Carleton University, Faculty of Engineering, Ottawa, Canada, 1996.

[2] Stimson, G. W.
Introduction to Airborne RADAR (2nd ed.).
Rayleigh, NC: Scitech Publishing, 1998.

[3] Gini, F., Farina, A., and Greco, M.
Selected list of references on radar signal processing.
IEEE Transactions on Aerospace and Electronic Systems, **37**, 1 (Jan. 2001), 329–359.

[4] Le Chevalier, F.
Principles of RADAR and SONAR Signal Processing.
Norwood, MA: Artech House, 2002.

[5] Rohling, H.
Some RADAR topics: Waveform design, range CFAR and target recognition.
In *NATO, Advanced Study Institute: Advances in sensing with security applications (Il Ciocco, Italy)*, Technical University Hamburg, Harburg, Germany, July 15–30, 2005.

[6] Shnidman, D. A.
Radar detection in clutter.
IEEE Transactions on Aerospace and Electronic Systems, **41**, 3 (July 2005), 1056–1067.

[7] Khalighi, M. and Bastani, M.
Adaptive CFAR processor for nonhomogeneous environments.
IEEE Transactions on Aerospace and Electronic Systems, **36**, 3 (July 2000), 889–897.

[8] Chen, B. and Varshney, P.
Adaptive CFAR detection for clutter-edge heterogeneity using Bayesian inference.
IEEE Transactions on Aerospace and Electronic Systems, **39**, 4 (Oct. 2003), 1470.

[9] Farrouki, A. and Barkat, M.
Automatic censoring CFAR detector based on ordered data variability for nonhomogeneous environments.
IEE Proceedings on Radar, Sonar, and Navigation, **152**, 1 (Feb. 2005), 43–51.

[10] Finn, H. M. and Johnson, P. S.
Adaptive detection mode with threshold control as a function of spatially sampled clutter estimation.
RCA Review, **29**, 3 (1968), 414–464.

[11] Alberola-López, C., Casar-Corredera, J. R., and de Miguel-Vela, G.
Object CFAR detection in gamma-distributed textured-background images.
IEE Proceedings on Vision, Signal and Image Processing, **146**, 3 (June 1999), 130–136.

[12] Gandhi, P. P. and Kassam, S. A.
Optimality of the cell averaging CFAR detector.
IEEE Transactions on Information Theory, **40**, 4 (July 1994).

[13] Swerling, P.
Probability of detection for fluctuating targets.
IEEE Transactions on Information Theory, **IT-6**, 2 (Apr. 1960), 269–308.

[14] Swerling, P.
Detection of RADAR echoes in noise revisited.
IEEE Transactions on Information Theory, **IT-12**, 3 (July 1966), 348–361.

[15] Swerling, P.
RADAR probability of detection for some additional fluctuating target cases.
IEEE Transactions on Aerospace and Electronic Systems, **33**, 2 (Apr. 1997), 698–709.

[16] Gandhi, P. P. and Kassam, S. A.
Analysis of CFAR processors in nonhomogeneous background.
IEEE Transactions on Aerospace and Electronic Systems, **24**, 4 (July 1988).

[17] Nitzberg, R.
Analysis of the arithmetic mean CFAR normalizer for fluctuating targets.
IEEE Transactions on Aerospace and Electronic Systems, **AES-1** (1978), 44–47.

[18] McConnell, I. and Oliver, C.
A comparison of segmentation methods with standard CFAR for point target detection.
SAR Image Analysis, Modelling and Techniques. In *Proceedings of SPIE*, vol. 3497, 1998, 76–87.

[19] McConnell, I. and Oliver, C.
Segmentation-based target detection in SAR.
SAR Image Analysis, Modelling and Techniques II. *Proceedings of SPIE*, vol. 3869, 1999, 45–54.

[20] Ndili, U., Nowak, R., Baraniuk, R., Choi, H., and Figueiredo, M.
Coding-theoretic approach to segmentation and a robust CFAR detector for LADAR images.
In *Algorithms for Synthetic Aperture Radar Imagery VIII. Proceedings of the SPIE 15th Annual International Symposium on Aerospace/Defense Sensing, Simulation, and Controls*, vol. 4382, Apr. 2001.

[21] Rohling, H.
RADAR CFAR thresholding in clutter and multiple target situations.
IEEE Transactions on Aerospace and Electronic Systems, **AES-19**, 4 (1983), 608–621.

[22] Trees, H. L. V.
Detection, Estimation, and Modulation Theory—Part I. Detection, Estimation, and Linear Modulation Theory.
New York: Wiley-Interscience, 2001.

[23] Abramowitz, M.
Handbook of Mathematical Functions.
New York: Dover, 1965.

[24] Bronshtein, I. and Semendyayev, K.
Handbook of Mathematics.
New York: Springer, 1997.

[25] Isar, A., Moga, S., and Isar, D.
A new method for denoising sonar images.
In *Proceedings of the International Symposium on Signals, Circuits and Systems*, vol. 2, July 2005, 469–472.

[26] Gradshteyn, I. S. and Ryzhik, I. M.
Table of Integrals Series and Products (6th ed.).
Burlington, MA: Academic Press, 2000.

[27] Press, W., Teukoisky, S., and Flannery, B.
Numerical Recipes in C (2nd ed.).
New York: Cambridge, 1973.

[28] Paranjape, R. B., Rabie, T. F., and Rangayyan, R. M.
Image restoration by adaptive-neighborhood noise subtraction.
Applied Optics, **33**, 14 (May 1994), 2861–2869.

[29] Rangayyan, R. M., Ciuc, M., and Faghih, F.
Adaptive-neighborhood filtering of images corrupted by signal-dependent noise.
Applied Optics, **37**, 20 (July 1998), 4477–4487.

[30] Vasile, G., Trouve, E., Lee, J. S., and Buzuloiu, V.
Intensity-driven adaptive-neighborhood technique for polarimetric and interferometric SAR parameters estimation.
IEEE Transactions on Geoscience and Remote Sensors, **44**, 6 (June 2006), 1609–1621.

[31] Papoulis, A.
Probability, Random Variables, and Stochastic Processes (3rd ed.).
New York: McGraw-Hill, 1991.

[32] Boccara, N.
Functional Analysis.
Boston, MA: Academic Press, 1990.

[33] Weiss, M.
Analysis of some modified cell-averaging CFAR processors in multiple-target situations.
IEEE Transactions on Aerospace and Electronic Systems, **AES-18** (Jan. 1982), 102–114.

[34] Acito, N., Corsini, G., Diani, M., and Pennucci, G.
Experimental performance analysis of clutter removal techniques in IR images.
IEEE International Conference on Image Processing, vol. 3, Sept. 2005.

[35] Moschopoulos, P. G.
The distribution of the sum of independent gamma random variables.
Annals of the Institute of Statistical Mathematics (Part A), **37** (1985), 541–544.

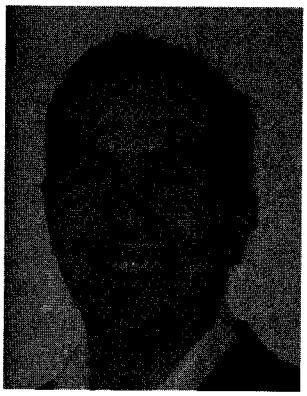

Éric Magraner graduated from École Nationale Supérieure de Physique de Marseille (ENSPM) in 2005. He is currently pursuing the Ph.D. in the Physics and Image Processing Group, Fresnel Institute (UMR CNRS 6133) and Paul Cézanne University.

His main research interests include detection and statistical techniques.

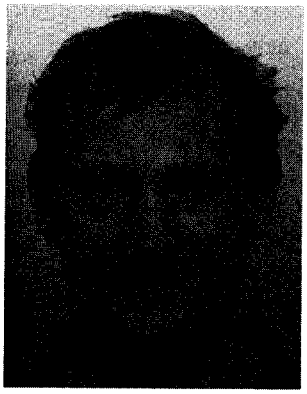

Nicolas Bertaux graduated from the École Normale Supérieure de Cachan. He received the M.Sc. degree in electrical engineering from Paris University, Orsay, France in 1993 and the "Agregation degree" in electrical engineering in 1994. He received the Ph.D. from Paris University in January 2000 in electrical engineering.

He is an assistant professor in electrical engineering at École Centrale de Marseille. His main research interests at Fresnel Institute (UMR CNRS 6133) include digital image processing and signal processing.

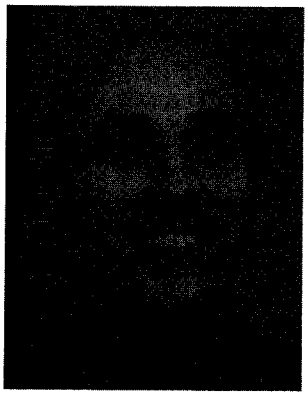

Philippe Réfrégier graduated from École Supérieure de Physique et Chimie Industrielles de la ville de Paris in 1984 and received the Ph.D. in solid state physics in 1987 from the University of Paris, Orsay.

He is a Full Professor of Signal Processing at École Centrale de Marseille. His present research interests at the Fresnel Institute (UMR CNRS 6133) include digital image and signal processing and statistical optics.